Study of Disorder in Different Phases of Tetratriacontane and a Binary Alkane Mixture, Using Vibrational Spectroscopy

P. A. Suranga R. Wickramarachchi,† Stephen J. Spells,* and D. Sujeewa M. de Silva†

Materials and Engineering Research Institute, City Campus, Sheffield Hallam University, Sheffield S1 1WB, U.K.

Received: September 22, 2006; In Final Form: December 13, 2006

Raman spectroscopy has been used to investigate the monoclinic crystal → rotator → melt phase transitions in *n*-$C_{34}H_{70}$, for both real-time heating and cooling runs. Changes in band intensity and frequency in the CH_2 bending, CH_2 twisting, skeletal C−C stretching, and CH_3 rocking regions revealed both transitions, particularly when using band components related to gauche bonds. In the room temperature infrared spectrum, the CH_2 rocking−twisting and CH_2 wagging progressions were observed and indexed for *n*-$C_{34}H_{70}$ and a 2:1 (w/w) mixture of $C_{34}H_{70}$ and $C_{36}D_{74}$. This led to best estimates for the all-trans crystal core in both cases of 33 to 34 carbon atoms, indicating that the core corresponds to almost the whole of the $C_{34}H_{70}$ molecule.

Introduction

Short chain *n*-alkanes are known to exhibit a range of crystal structures, depending on both the number of carbon atoms in the chain and whether this number is odd or even. While odd *n*-alkanes up to C_{39} show an orthorhombic structure, even alkanes below C_{26} have a triclinic structure. Those with 26 or more carbon atoms adopt a monoclinic form with an orthorhombic subcell. The present work concerns one of the last group, *n*-$C_{34}H_{70}$. Use is made of Raman spectroscopy to study phase transitions and, in particular, those involving the rotator phase. This forms part of an ongoing wider study of the structures of long chain *n*-alkanes, where crystal phases incorporate varying degrees of disorder. By combining, for the first time, information obtained from different regions of the Raman spectrum for a single material, we aim to establish whether Raman spectroscopy can provide a suitable technique for identifying the rotator phase during real-time heating and cooling runs on *n*-$C_{34}H_{70}$, before applying the technique to long alkanes. To our knowledge, such experiments have not been carried out previously in real time. We also make use of a microspectroscopic technique to help ensure a uniform sample temperature. In addition, progression bands in the infrared spectrum are used to characterize chain regularity in $C_{34}H_{70}$ by comparison with a binary mixture of $C_{34}H_{70}$ and $C_{36}D_{74}$. The use of a deuterated component also opens the possibility of utilizing progression bands for this molecule.

$C_{34}H_{70}$ transforms from its low temperature monoclinic crystal to an orthorhombic structure at 69.2 °C.[1] The orthorhombic-to-rotator phase transition is at 69.6 °C, followed by melting at 72.9 °C. In general, orthorhombic and monoclinic crystal structures give rise to crystal field splittings in both CH_2 rocking and bending modes.[2] Boerio and Koenig reported such splittings in the Raman CH_2 bending mode of several crystal structures in short *n*-alkanes.[3] Three other regions of the Raman spectrum show conformational sensitivity. First, Kim et al. studied conformationally sensitive CH_3 rocking vibrations in the 830−900 cm^{-1} region of the Raman spectrum of $C_{21}H_{44}$, $C_{50}H_{102}$, and a binary mixture of $C_{46}H_{94}$ and $C_{50}H_{102}$.[4] Components were observed in the rotator phase at frequencies close to those calculated at 892 cm^{-1} (tt), 879 cm^{-1} (gt), 862 cm^{-1} (gg), and 850 cm^{-1} (tg). The second region concerns the CH_2 twisting mode, which has two components in the Raman spectrum: a crystalline band at 1295 cm^{-1} and a counterpart arising from gauche bonds at 1305 cm^{-1}.[5] A slight broadening of the 1295 cm^{-1} line occurs with increasing conformational disorder in polyethylene, while the melt spectrum is dominated by the broad 1305 cm^{-1} band. Because of the highly localized character of the vibration, Strobl and Hagedorn suggest that the total Raman intensity should be independent of chain conformation and have shown experimentally that this is the case.[6] The final region showing conformational sensitivity is the C−C stretching region. Here, two strong bands at 1060 and 1130 cm^{-1} arise from trans C−C bonds and a broad band centered around 1080 cm^{-1} is due to gauche conformers.[5,7] The intensity of this last band increases with increasing temperature, whereas the two strong bands become progressively weaker. The melt spectrum is dominated by the 1080 cm^{-1} band.

The rotator phase, occurring just below the melting point in *n*-alkanes, has been studied by a range of techniques, including X-ray scattering,[8−13] neutron scattering,[14,15] infrared and Raman spectroscopy,[16−19] NMR,[20−23] and dielectric absorption.[24] Here, we will briefly review the vibrational spectroscopic studies. The disappearance of the correlation splitting of the CH_2 bending and rocking modes at the phase transition has been investigated.[18,25] In addition, the increase in chain disorder at the phase transition has been widely studied by infrared spectroscopy,[16,26−28] primarily using localized CH_2 wagging modes. Maissara and Devauve have reported the use of CH_3 rocking modes in the Raman spectrum to quantify the levels of disorder in several short *n*-alkanes in the rotator phase,[29] while Kim et al. observed the same conformationally sensitive bands in *n*-$C_{21}H_{44}$[4] and $C_{50}H_{102}$.[28] In addition, a second set of bands assigned to a CH_2 rocking progression were observed in the rotator phase but not for the ordered crystalline state.[4] Kurelec et al. have focused on the C−C skeletal bands in the 1000−1200 cm^{-1} region and the CH_2 bending region to characterize phase transitions in

* To whom correspondence should be addressed.
† Current address: Department of Chemistry, University of Kelaniya, Kelaniya, Sri Lanka.

10.1021/jp066207h CCC: $37.00
Published on Web 01/26/2007

ultrahigh molecular weight polyethylene (UHMW-PE),[30] using in situ Raman spectroscopy as a function of temperature and pressure. We wish to evaluate the information available from all of the Raman spectral regions listed above, in the context of real-time heating and cooling experiments on a single short alkane, *n*-$C_{34}H_{70}$. The results will provide a basis for similar future measurements on phase transitions in long alkanes, and particularly for those involving highly disordered phases.

Nonlocalized progression bands in the infrared spectra of alkanes also show a remarkable conformational sensitivity. The rocking−twisting (P_k), C−C stretching (R_k), and CH_2 wagging (W_k) progressions can all be used for the identification of phase transitions. Frequency−phase relationships were determined by Snyder and Schachtschneider for short alkanes from *n*-$C_{20}H_{42}$ to *n*-$C_{30}H_6$.[31] The phase difference between motions of adjacent methylene groups along the chain for a particular vibration, φ_k, is related to the number of carbon atoms, n_C, through the integer *k*:

$$\varphi_k = \frac{k\pi}{n_C - 1} \quad (1)$$

where n_C represents the all-trans chain length. In the infrared spectrum of an all-trans chain, only *k*-odd members of the progression are observed, while *k*-even members are forbidden.[31] The development of chain end disorder, and resultant change in chain symmetry, activates the *k*-even series, with increasing intensity at the expense of the intensity of *k*-odd modes as the temperature increases. The opposite situation is found in Raman spectroscopy, with only the *k*-even series obtained for the all-trans chain.[4]

Snyder and co-workers have used the *k*-even components to demonstrate the high temperature rotator phase of short chain alkanes.[26,32] The CH_2 rocking−twisting mode at low temperatures shows a well separated progression from 720 to 1030 cm^{-1} in the infrared spectrum, with only *k*-odd modes visible. In the rotator phase, both *k*-odd and *k*-even progressions are seen. Frequency and intensity calculations have shown that the new sequence is associated with an end-gauche conformation in an otherwise planar molecule.[26] Gorce and Spells used the C−C stretching/CH_2 twisting progression to demonstrate the "perfecting" of *n*-$C_{198}H_{398}$ crystals with annealing.[33] The regularity of progression bands was found to improve markedly with heat treatment, and the conclusions are supported by studies of the CH_2 wagging modes[34] and, in the case of isotopically labeled long alkanes, the CD_2 bending vibration.[35] Indexing progression bands, with the aid of eq 1 above, allows the all-trans chain length to be determined. This was carried out for *n*-$C_{198}H_{398}$, *n*-$C_{246}H_{494}$, a center-branched long alkane, and a binary mixture of *n*-$C_{162}H_{326}$ and *n*-$C_{246}H_{494}$.[33] The results were consistent with the relevant structures—extended chain, once-folded, and a triple layer superlattice. In the present work, we use progression bands to compare the core thickness of the crystals in $C_{34}H_{70}$ and the binary mixture $C_{34}H_{70}/C_{36}D_{74}$ to characterize any differences in the degree of order present.

Experimental Section

n-$C_{34}H_{70}$ was obtained from Sigma Chemicals, with 99% purity. *n*-$C_{36}D_{74}$ with 98% purity was obtained from the Aldrich Chemical Co., as was spectrophotometric grade toluene (99.5%). A mixture of $C_{34}H_{70}$ and $C_{36}D_{74}$ was prepared (2:1 w/w), by dissolution in hot toluene. After crystallization on cooling, the filtered and dried crystals were melted several times to ensure homogeneous mixing and pressed to obtain a thin film. A similar film of $C_{34}H_{70}$ was prepared.

For Raman measurements, approximately 3 mg of as-obtained crystals was placed in the lid of a Mettler DSC pan, which formed the sample holder. A disc of aluminum foil, of marginally larger diameter than the pan, was used as the lid, and a 2 mm diameter hole was made for both incoming and outgoing light paths. This helped to ensure a uniform temperature over the sampled area. A Renishaw Ramascope 2000 spectrometer was used to record conventional Raman spectra with the 785 nm line of a diode laser for excitation. The stigmatic single spectrograph was attached to an Olympus BH2 microscope and made use of a Peltier-cooled CCD detector. A 20× microscope objective was used. The spectral resolution was approximately 2 cm^{-1}, and spectra were recorded between 150 and 1700 cm^{-1}. A Linkam microscope hot stage was used for heating and cooling experiments, with a rate of 5 °C min^{-1} between periods of data collection. The Raman spectra were recorded at every 1 °C, with typical data collection times up to 50 s. The analysis of the Raman spectra involved baseline correction and curve fitting procedures, using GRAMS 32 software.

Fourier transform infrared (FTIR) transmission spectra were obtained using a Mattson Galaxy 6020 spectrometer with an MCT detector. The sample was held in a Graseby-Specac 21500 cryostat, controlled with a 20120 temperature controller. The sample space of the cryostat was evacuated. The spectral resolution was 1 cm^{-1}, and 200 scans were used for each spectrum. Curve fitting was carried out using GRAMS software.

To facilitate heating and cooling runs involving the molten state, attenuated total reflection (ATR)−FTIR measurements were undertaken using a Nicolet Magna 860 spectrometer. This was equipped with a Graseby-Specac single reflection diamond crystal accessory, allowing sample heating. Temperature calibration was performed with samples of tetratriacontane (Sigma Chemicals, 99%), tetratetracontane (Aldrich Chemicals, 99%), glutaric acid (Aldrich, 99%), hexadecanedioic acid (Aldrich, 96%), and suberic acid (Aldrich, 98%). The spectral resolution was 1 cm^{-1}, and typically, 64 sample scans were used.

Raman Spectroscopy

The spectrum of $C_{34}H_{70}$ will be considered in terms of four spectral regions, as outlined in the Introduction: (i) the complex 1400−1500 cm^{-1} CH_2 bending region, (ii) the CH_2 twisting vibration around 1300 cm^{-1}, (iii) the C−C skeletal vibrations between 1000 and 1200 cm^{-1}, and (iv) the CH_3 rocking region, around 890 cm^{-1}.

(i) CH_2 Bending Region (1400−1500 cm^{-1}). This region is somewhat complicated by combination bands and overtones. Nevertheless, a well resolved triplet can be identified at 1418, 1438, and 1460 cm^{-1}. There is no doubt concerning the assignment of the two narrow bands at 1418 and 1438 cm^{-1} as the CH_2 bending doublet.[3,6] The 1460 cm^{-1} band arises from overtones and combinations in Fermi resonance with the fundamental at 1438 cm^{-1}. Boerio and Koenig reported the dependence of the 1418 cm^{-1} band on crystal structure, with the band only being observed for orthorhombic and monoclinic forms.[3] Selected data, collected as a function of temperature, are shown in Figure 1 for *n*-$C_{34}H_{70}$. The disappearance of the 1418 cm^{-1} band, denoted by a star, marks the transition from the monoclinic phase to the rotator phase, in agreement with the observations of Boerio and Koenig. The 1460 and 1438 cm^{-1} bands are still resolved in the rotator phase, although a small shift was observed in the 1460 cm^{-1} band at the phase transition. In the melt, a broad band was observed, centered at 1438 cm^{-1}, with a broad shoulder around 1460 cm^{-1}.

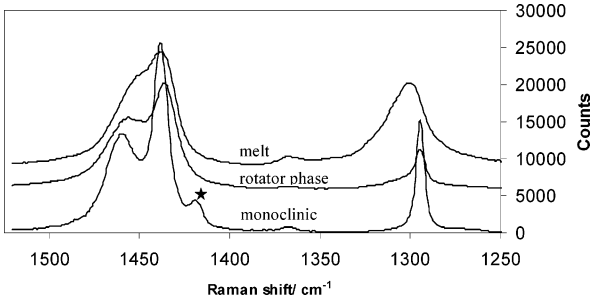

Figure 1. CH_2 bending and twisting region of the Raman spectrum of $C_{34}H_{70}$ in monoclinic, rotator, and melt phases at 62, 71, and 76 °C, respectively.

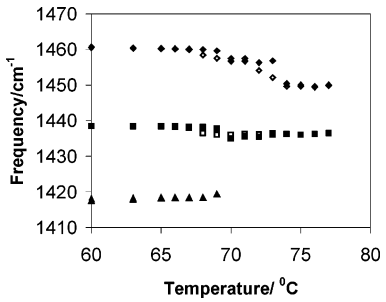

Figure 2. Changes in the band positions of the Raman CH_2 bending triplet with temperature. Open symbols indicate a heating run, and closed symbols refer to cooling.

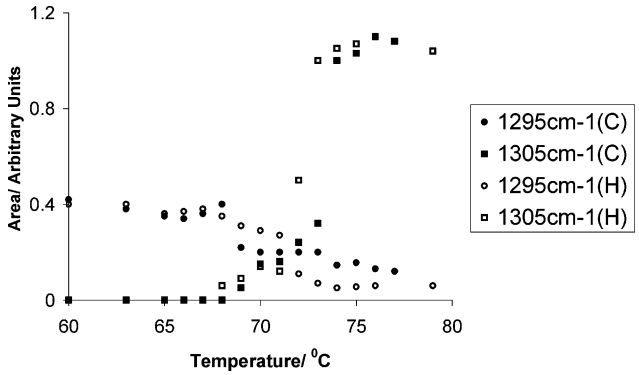

Figure 3. Variation in the area of the Raman 1295 and 1305 cm^{-1} bands with temperature. Open symbols indicate a heating run (H), and closed symbols cooling (C).

Curve fitting was used to measure the changes in band positions for the bending triplet observed in Figure 1, and the results are shown in Figure 2. The monoclinic-to-rotator phase transition is marked by shifts in both 1438 and 1460 cm^{-1} bands, at 67 °C during heating and at 69 °C on cooling. Similarly, the 1418 cm^{-1} band disappears/appears at the same temperatures. The 1460 cm^{-1} band shows a second step in frequency at 71−74 °C on heating and 73−74 °C on cooling. We identify this with melting of the rotator phase.

(ii) CH_2 Twisting Region (around 1300 cm^{-1}). As illustrated in Figure 1, $C_{34}H_{70}$ shows only a narrow peak at 1295 cm^{-1} in the monoclinic phase. An asymmetric broadening in the rotator phase indicates a contribution from the 1305 cm^{-1} band, resulting from conformationally disordered chains. In the melt, the broad 1305 cm^{-1} band dominates. Changes in the areas of the two components with temperature are shown in Figure 3. There is no sign of the 1305 cm^{-1} band until 68 °C on heating, and the band disappears at 68 °C on cooling. This appearance/disappearance of the 1305 cm^{-1} band coincides with a reduction/increase in the area of the 1295 cm^{-1} band, marking the phase

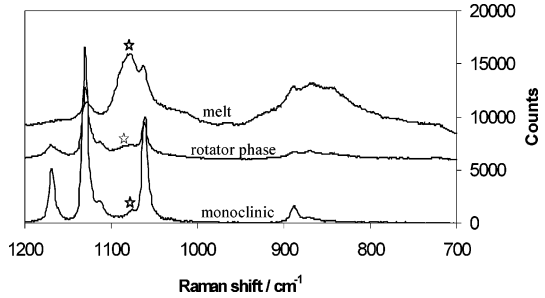

Figure 4. C−C stretching and CH_3 rocking modes of $C_{34}H_{70}$ for different phases at 62, 71, and 76 °C, respectively.

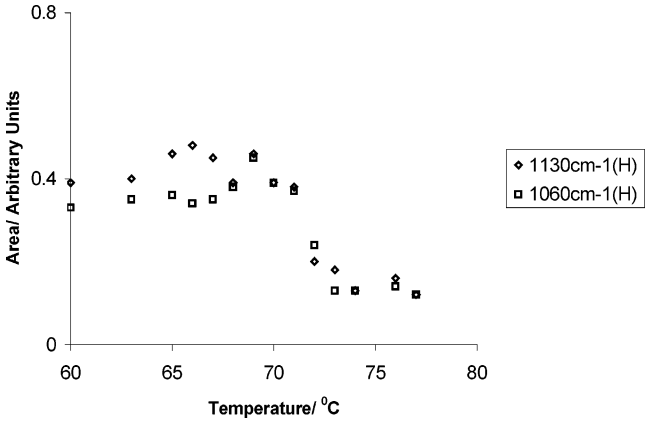

Figure 5. Areas of the Raman 1130 and 1060 cm^{-1} C−C skeletal modes of $C_{34}H_{70}$ as a function of temperature during a heating run.

transition between monoclinic and rotator phases at 68 °C. Within the rotator phase, the behavior of the 1295 cm^{-1} component differs somewhat on heating and cooling. On cooling, the area remains reasonably constant as a function of temperature. On heating, the area progressively decreases. In both experiments, the 1305 cm^{-1} band area increases slightly with increasing temperature through the rotator phase. Melting is indicated by a large increase in the area of the 1305 cm^{-1} band at 72−73 °C (73−74 °C on cooling). A reduction in the area of the 1295 cm^{-1} band was observed on heating at 71−72 °C, but the transition was less clear (73−74 °C) on cooling. Clearly, a proportion of short all-trans sequences is retained in the rotator phase and a smaller, but not negligible, proportion in the melt.

(iii) Skeletal C−C Stretching Mode (1000−1150 cm^{-1}). Figure 4 shows the Raman spectrum of $C_{34}H_{70}$ in this region. The relevant bands are at 1060, 1080 (marked by a star), and 1130 cm^{-1}. The 1080 cm^{-1} band shows a large increase in intensity on melting, while there are still signs of the 1060 and 1130 cm^{-1} bands in the melt.

Figure 5 shows the areas of the crystalline components as a function of temperature, on heating the sample. A decrease in area in the region 71−73 °C indicates melting, but there is no sign of the monoclinic-to-rotator phase transition. Corresponding data for a cooling run did not show either transition clearly. The behavior of the 1080 cm^{-1} band due to gauche conformers is seen in Figure 6, for both heating and cooling runs. An increase in intensity at 67−68 °C on heating (see open circles, using expanded scale) marks the monoclinic-to-rotator phase transition. The major change in intensity at the melting transition occurs at 72−73 °C on heating (73−74 °C on cooling). The intensity also changes significantly with the temperature in the melt, behavior which is to be expected for a band purely related to the number of gauche bonds, rather than to particular bond sequences involving gauche bonds.

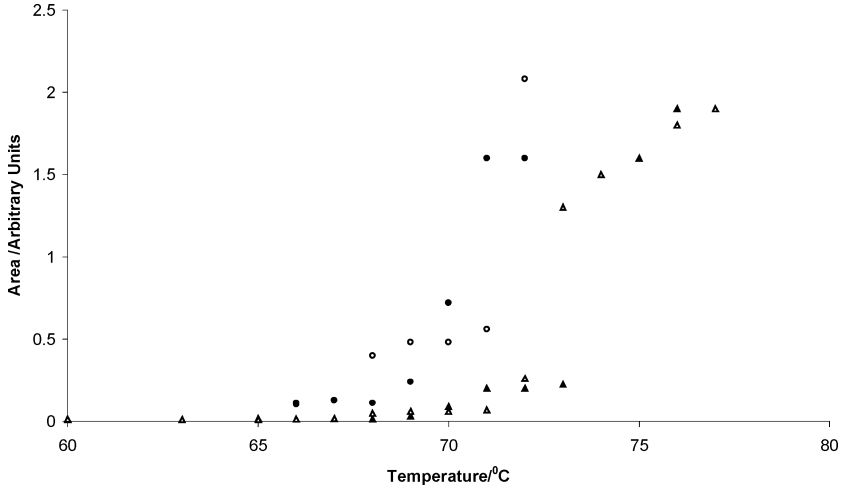

Figure 6. Area of the Raman 1080 cm^{-1} C−C skeletal mode of $C_{34}H_{70}$ versus temperature. Filled and unfilled triangles refer to cooling and heating runs, respectively, while filled and unfilled circles show data on an expanded (×8) scale.

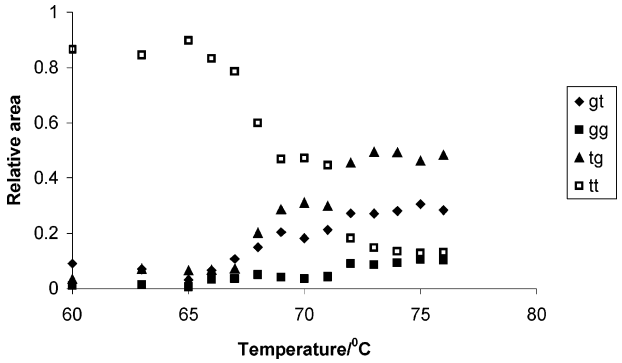

Figure 7. Variation with temperature of the relative areas of the Raman CH_3 rocking band components arising from different bond conformations.

(iv) CH_3 Rocking Modes (Approximately 890 cm^{-1}). Figure 4 includes this region of the spectrum. The assignment of individual bands to specific bond pairs has been described in the Introduction. All four bands have been identified in these spectra. In the monoclinic crystal form, the tt component at 892 cm^{-1} is dominant. The rotator phase shows appreciable intensity for conformations involving a gauche bond, and the intensities of these bands further increase in the melt. The spectrum of the melt shows a very broad feature, with some components still resolved.

The relative intensities of the different components are shown in Figure 7. On heating, the intensity for all bond sequences involving a gauche bond starts to increase at 67 °C, with the midpoint in the transition occurring close to 68 °C. This clearly marks the monoclinic-to-rotator phase transition. The increase in intensity for the gg component (862 cm^{-1}) is smaller than that for the gt and tg bands, indicating the small probability of adjacent gauche bonds. The corresponding reduction in intensity of the tt component (892 cm^{-1}) occurs at 67−69 °C. The melting transition is marked by a further reduction in the 892 cm^{-1} band intensity and an increase in intensity of all other components at 71−72 °C. In contrast with Figure 6, the relative proportions of the band intensities due to gauche-containing sequences here stay reasonably constant in the melt as a function of temperature.

Infrared Spectroscopy

(i) $C_{34}H_{70}$. Figures 8 and 9 show the methylene rocking−twisting and methyl wagging progressions in the infrared spectrum at room temperature. The assignment of values for

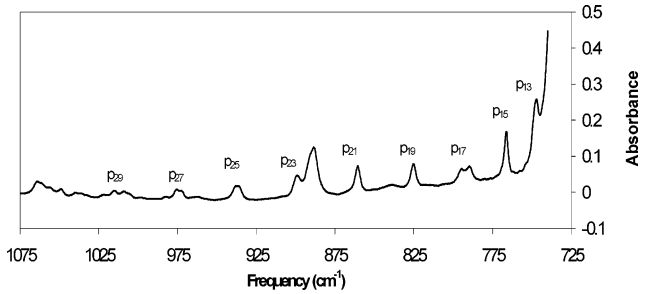

Figure 8. Infrared methylene rocking−twisting progression of $C_{34}H_{70}$ at room temperature.

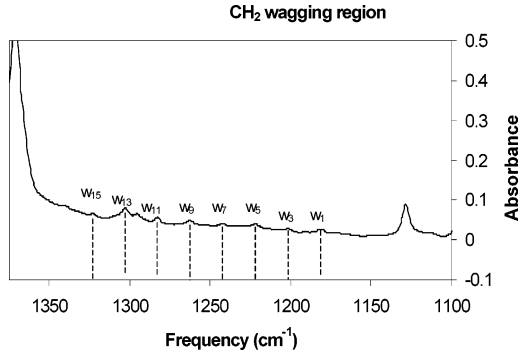

Figure 9. Infrared methylene wagging progression of $C_{34}H_{70}$ at room temperature.

the integer k in eq 1 above followed the same procedure as previously for n-$C_{44}H_{90}$[36] and for long alkanes.[33] The method will briefly be described here. First, the frequency of each progression band component was identified and the corresponding phase difference (φ_k/π) was determined from the frequency−phase curves of Snyder and Schachtschneider.[31] The value for the number of carbon atoms, n_C, in eq 1 was initially set at 34. This represents the largest possible all-trans length for this molecule. Equation 1 was then used to calculate a series of k values for the observed bands. This procedure was repeated for different estimates of n_C, corresponding to shorter all-trans chain lengths. The iteration providing the closest match to a sequence of odd integers for the calculated k values was then chosen as the best fit, and the n_C value used is listed, for example, in column 3 of Table 1. By rounding off the calculated k values to odd integers, values of n_C could then be calculated, again using eq 1, and an average value of n_C could be obtained as the best estimate of the all-trans chain length. Such figures are given

TABLE 1: Indexation of *k* Values for the CH_2 Rocking/Twisting Progression of $C_{34}H_{70}$ and Calculation of an Average Value for n_C

frequency (cm^{-1})	φ_k/π	*k* values for $n_C = 33$	rounded values for *k*	n_C values calculated from rounded values for *k*
746.9	0.415	13.280	13	32.33
766.0	0.464	14.848	15	33.33
789.4	0.523	16.736	17	33.50
825.0	0.590	18.884	19	33.20
860.6	0.649	20.768	21	33.36
899.1	0.708	22.656	23	33.49
937.6	0.774	24.768	25	32.45
972.3	0.834	26.688	27	33.26
1014.8	0.911	28.896	29	33.12
		average value for n_C:		33.12

in the fifth column of Table 1. The rocking−twisting progression gave the best fit unambiguously for $n_C = 33$, with the *k* values noted in Figure 8. The average value of 33.12 for n_C indicates an all-trans chain length of almost one carbon atom less than the whole molecule. The wagging progression showed some ambiguity in the results, with both $n_C = 33$ and $n_C = 34$ giving a good fit to the *k* values shown in Figure 9. The average value of 33.44 reveals the reason for this ambiguity, being approximately midway between the two integers.

Figure 10 shows the variation of the rocking−twisting progression with increasing temperature, from ATR−FTIR measurements. In the lowest temperature spectrum (55 °C), *k*-odd bands (located using the vertical dotted lines) are prominent. On entering the rotator phase (68 °C), the formation of end-gauche defects with an associated loss of symmetry activates the *k*-even components, although the *k*-odd components retain a higher intensity. At 72 °C, the relative intensity of the *k*-even series increases at the expense of that of the *k*-odd series. The melt spectrum at 76 °C shows only broad features in this region, with neither odd nor even series components resolved. Unfortunately, the quality of the progression band data in the rotator phase precludes detailed analysis, although the similarity in *k*-odd band positions at 55 and 68 °C (and also at 72 °C) suggests little change in the all-trans length.

(ii) $C_{34}H_{70}/C_{36}D_{74}$ Mixture. With the mismatch in chain length in this 2:1 (w/w) mixture, we consider the possibility that the deuterated chains assume an end-gauche conformation. The alternative is a "kink" in the middle of the chain to shorten its length.

Infrared spectra in the rocking−twisting and wagging region are shown in Figures 11 and 12, and these again show characteristic progressions. The same method was used to assign

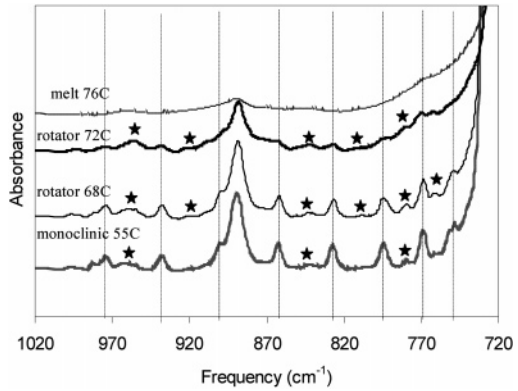

Figure 10. Infrared (ATR−FTIR) methylene rocking−twisting progression for different phases of $C_{34}H_{70}$. Dashed lines represent the *k*-odd bands.

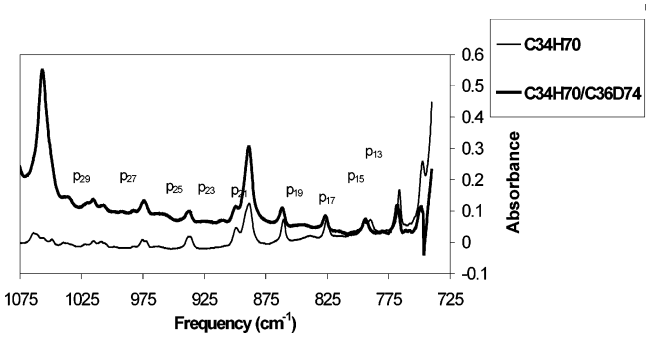

Figure 11. Infrared methylene rocking−twisting progression of the $C_{34}H_{70}/C_{36}D_{74}$ mixture compared with that of $C_{34}H_{70}$.

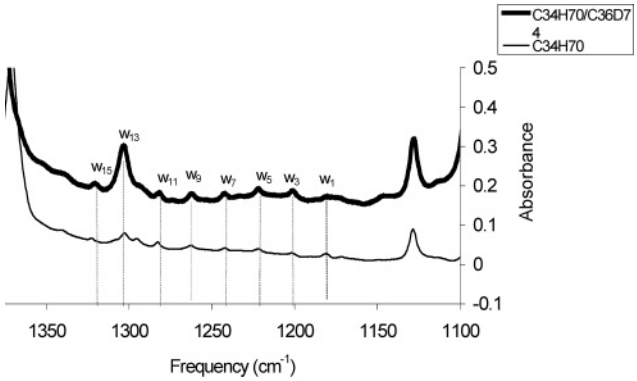

Figure 12. Infrared methylene wagging progression of the $C_{34}H_{70}/C_{36}D_{74}$ mixture compared with that of $C_{34}H_{70}$.

TABLE 2: Indexation of *k* Values for the CH_2 Wagging Progression of $C_{34}H_{70}$ and Calculation of an Average Value for n_C

frequency (cm^{-1})	φ_k/π	*k* values for $n_C = 33$	*k* values for $n_C = 34$	rounded values for *k*	n_C values calculated from rounded values for *k*
1181.1	0.032	1.024	1.056	1	32.25
1201.9	0.092	2.994	3.036	3	33.61
1221.8	0.153	4.896	5.049	5	33.68
1242.3	0.217	6.994	7.161	7	33.26
1262.5	0.277	8.864	9.141	9	33.49
1283.1	0.338	10.816	11.154	11	33.54
1302.5	0.396	12.672	13.068	13	33.83
1322.8	0.456	14.592	15.048	15	33.89
			average value for n_C:		33.44

TABLE 3: Indexation of *k* Values for the CH_2 Rocking/Twisting Progression of a $C_{34}H_{70}/C_{36}D_{74}$ Mixture and Calculation of an Average Value for n_C

frequency (cm^{-1})	φ_k/π	*k* values for $n_C = 33$	rounded values for *k*	n_C values calculated from rounded values for *k*
748.4	0.418	13.794	13	32.10
767.9	0.479	15.328	15	32.32
793.6	0.533	17.056	17	32.89
826.4	0.592	18.944	19	33.09
861.7	0.654	20.928	21	33.11
899.2	0.708	22.656	23	33.49
937.8	0.774	24.768	25	33.3
974.4	0.837	26.784	27	33.26
1015.3	0.911	29.152	29	32.83
		average value for n_C:		32.93

progression bands as for $C_{34}H_{70}$ alone. The "best fits" to values of n_C are shown in Tables 3 and 4.

As previously found for *n*-$C_{34}H_{70}$, analysis of the rocking−twisting progression shows that $n_C = 33$ provides the best fit, with an averaged value of $n_C = 32.93$. For the wagging

TABLE 4: Indexation of *k* Values for the CH_2 Wagging Progression of a $C_{34}H_{70}/C_{36}D_{74}$ Mixture and Calculation of an Average Value for n_C

frequency (cm^{-1})	φ_k/π	*k* values for $n_C = 33$	*k* values for $n_C = 34$	rounded values for *k*	n_C values calculated from rounded values for *k*
1180.9	0.030	0.96	0.99	1	34.33
1201.7	0.090	2.88	2.97	3	34.33
1222.0	0.153	4.90	5.05	5	33.68
1241.9	0.215	6.88	7.10	7	33.56
1262.2	0.273	8.74	9.01	9	33.97
1282.1	0.335	10.72	11.06	11	33.83
1303.8	0.400	12.80	13.20	13	33.50
1321.0	0.454	14.53	14.98	15	34.04
			average value for n_C:		33.91

progression, both $n_C = 33$ and 34 provide good fits to the data, with the same *k* values. The fit is rather better for $n_C = 34$, as confirmed by the averaged value of $n_C = 33.91$. Interestingly, by comparison with the $C_{34}H_{70}$ sample, the averaged n_C is slightly smaller here for the rocking−twisting progression and rather larger for the wagging progression. Nevertheless, the all-trans chain lengths derived for the two samples are sufficiently similar to suggest that the crystal core has the same structure, namely, an almost fully extended $C_{34}H_{70}$ chain. It follows that the deuterated chain ends adopt an end-gauche conformation outside the crystal core.

The close correspondence in the positions of progression bands for the pure alkane and the binary mixture (Figures 11 and 12) demonstrates that these bands are solely related to the $C_{34}H_{70}$ molecule. No progressions were found corresponding to the deuterated molecule.

Discussion and Conclusions

Several regions of the Raman spectrum were found to provide clear indications of the monoclinic-to-rotator phase transition in *n*-$C_{34}H_{70}$ during real-time heating and cooling runs. This demonstrates the sensitivity of Raman spectroscopy to relatively small changes in structural disorder, a feature which has potential applications in studying the more complex phase behavior of long alkanes. Evidence for the phase transition comes from changes in intensity in both crystalline bands and those due to gauche conformers. In the CH_2 bending region, the 1418 cm^{-1} band disappears at this phase transition and both the 1438 and 1460 cm^{-1} bands show frequency shifts. The CH_2 twisting region shows an intensity reduction in the crystalline 1295 cm^{-1} peak and an increase in the 1305 cm^{-1} band arising from gauche bonds. In the skeletal C−C stretching region, crystalline bands at 1060 and 1130 cm^{-1} were relatively insensitive to the transition, while the 1080 cm^{-1} band due to gauche conformers showed a clear increase in intensity at the phase transition. CH_3 rocking bands due to different bond conformations revealed the transition quite clearly, with intensity increases for conformations including a gauche bond and an intensity decrease for the band due to tt conformers. In summary, the CH_2 bending and CH_3 rocking regions can be said to reveal the transition most clearly and may prove to be the most useful in applications involving long alkanes. However, the lower concentration of methyl groups may restrict the choice. The behaviors of the different Raman bands also display differences within the phases observed. Particularly noticeable is the increase in intensity of the 1080 cm^{-1} band within the melt state with increasing temperature. This probably relates to its origins in individual gauche bonds.

The onset of the rotator phase is also apparent in the CH_2 rocking−twisting progression of the infrared spectrum, with *k*-even components appearing at the expense of *k*-odd bands. Both rocking−twisting and wagging progressions were indexed and used to obtain estimates of the core all-trans chain length in $C_{34}H_{70}$ and a binary mixture with $C_{36}D_{74}$, at room temperature. In both cases, best fits were obtained using 33 or 34 as the number of carbon atoms in the all-trans core, indicating that most of the $C_{34}H_{70}$ molecule forms the crystalline core. The additional bonds in $C_{36}D_{74}$ are thus believed to be excluded from the core, in end-gauche conformations. No indication was seen of independent band progressions arising from the deuterated molecule.

It should be noted that most of the types of behavior observed here in Raman and infrared spectra have, individually, been previously reported for different *n*-alkanes. In the present work, the techniques are brought together and evaluated. We have also demonstrated the practicality of real-time Raman measurements during heating and cooling.

Acknowledgment. We wish to thank Professor Goran Ungar and Dr. Xiang-Bing Zeng (University of Sheffield) for useful discussions. We are also indebted to Dr. Chris Sammon for assistance with the Raman and ATR−FTIR measurements.

References and Notes

(1) Broadhurst, M. G. *J. Res. Natl. Bur. Stand. (U.S.)* **1962**, *66A*, 241.
(2) Cutler, D. J.; Hendra, P. J.; Walker, J. H.; Cudby, M. E. A.; Willis, H. A. *Spectrochim. Acta* **1978**, *34A*, 391.
(3) Boerio, F. J.; Koenig, J. L. *J. Chem. Phys.* **1970**, *52* (7), 3425.
(4) Kim, Y.; Strauss, H. L.; Snyder, R. G. *J. Phys. Chem.* **1989**, *93*, 485.
(5) Naylor, C. C.; Meier, R.; Kip, B. J.; Williams, P. J.; Mason, S. M.; Conroy, N.; Gerrard, D. L. *Macromolecules* **1995**, *28*, 2969.
(6) Strobl, G. R.; Hagedorn, W. *J. Polym. Sci., Polym. Phys. Ed.* **1978**, *16*, 1181.
(7) Tarazona, A.; Koglin, E.; Coussens, B.; Meier, R. J. *Vib. Spectrosc.* **1997**, *14*, 159.
(8) Müller, A. *Proc. R. Soc. (London), Ser. A* **1930**, *127*, 417.
(9) Piesczek, W.; Strobl, G. R.; Malzahn, K. *Acta Crystallogr.* **1974**, *B30*, 1278.
(10) Larsson, K. *Nature* **1967**, *28*, 383.
(11) Doucet, J.; Denicolo, I.; Craievich, A. *J. Chem. Phys.* **1981**, *75*, 1523.
(12) Ungar, G. *J. Phys. Chem.* **1983**, *87*, 689.
(13) Craievich, A.; Denicolo, I.; Doucet, J. *Phys. Rev. B* **1984**, *30*, 4782.
(14) Barnes, J. D. *J. Chem. Phys.* **1973**, *58*, 5193.
(15) Doucet, J.; Dianoux, A. J. *J. Chem. Phys.* **1984**, *81*, 5043..
(16) Maroncelli, M.; Qi, S. P.; Strauss, H. L.; Snyder, R. G. *J. Am. Chem. Soc.* **1982**, *104*, 6237.
(17) Nielsen, J. R.; Hathaway, C. E. *J. Mol. Spectrosc.* **1963**, *10*, 366.
(18) Barnes, J. D.; Fanconi, B. M. *J. Chem. Phys.* **1972**, *56*, 5190.
(19) Zerbi, G.; Magni, R.; Gussoni, M.; Moritz, K. H.; Bigotto, A.; Dirlikov, S. *J. Chem. Phys.* **1950**, *58*, 252.
(20) Dehl, R. E. *J. Chem. Phys.* **1973**, *60*, 339.
(21) Olf, H. G.; Peterlin, A. *J. Polym. Sci., Part A* **1970**, *8*, 753.
(22) Ewen, B.; Fischer, E. W.; Piesczek, W.; Strobl, G. *J. Chem. Phys.* **1974**, *61*, 5265.
(23) Stohrer, M.; Noack, F. *J. Chem. Phys.* **1952**, *20*, 541.
(24) Chapman, D.; Wallach, D. F. H. *Biological Membranes*; Academic Press: London, 1968 and 1973; Vols. I and II.
(25) Ungar, G.; Masic, N. *J. Phys. Chem.* **1985**, *89*, 1036.
(26) Snyder, R. G.; Maroncelli, M.; Qi, S. P.; Strauss, H. L. *Science* **1981**, *214*, 188.
(27) Maroncelli, M.; Strauss, H. L.; Snyder, R. G. *J. Phys. Chem.* **1985**, *89*, 5260.
(28) Kim, Y.; Strauss, H. L.; Snyder, R. G. *J. Phys. Chem.* **1989**, *93*, 7520.
(29) Maissara, M.; Devaure, J. *J. Raman Spectrosc.* **1987**, *18*, 181.
(30) Kurelec, L.; Rastogi, S.; Meier, R. J.; Lemstra, P. J. *Macromolecules* **2000**, *33*, 5593.
(31) Snyder, R. G.; Schachtschneider, J. H. *Spectrochim. Acta.* **1963**, *19*, 85.
(32) Maroncelli, M.; Qi, S. P.; Strauss, H. L.; Snyder, R. G. *J. Am. Chem. Soc.* **1982**, *104*, 6237.
(33) Gorce, J.-P.; Spells, S. J. *Polymer* **2002**, *43*, 4043.
(34) Gorce, J.-P.; Spells, S. J. *Polymer* **2004**, *45*, 3297.
(35) De Silva, D. S. M.; Gorce, J.-P.; Wickramarachchi, P. A. S. R.; Spells, S. J. *Macromol. Symp.* **2002**, *184*, 67.
(36) Gorce, J.-P.; Spells, S. J.; Zeng, X.-B. and Ungar, G. *J. Phys. Chem. B* **2004**, *108*, 3130.